Propagation of Interacting Cracks in Offshore Wind Welded Structures Through Numerical Analysis

Mishael, Jose; Morato, Pablo G.; Rigo, Philippe

Publication date
2024

Document Version
Final published version

Published in
Proceedings of the Thirty-fourth (2024) International Ocean and Polar Engineering Conference

Proceedings of the Thirty-fourth (2024) International Ocean and Polar Engineering Conference **www.isope.org**
Rhodes, Greece, June 16–21, 2024

ISBN 978-1-880653-78-4; ISSN 1098-6189

Propagation of Interacting Cracks in Offshore Wind Welded Structures through Numerical Analysis

Jose Mishael[1], Pablo G. Morato[2], Philippe Rigo[1]

[1]ANAST, ArGEnCo, University of Liege
Liege, Belgium

[2]Faculty of Architecture and the Built Environment,
Delft University of Technology
Delft, Netherlands

ABSTRACT

This study investigates the behavior of interacting surface cracks at the circumferential weld toe of monopile-supported offshore wind turbines. Relying on a numerical model that explicitly considers weld profiles, we explore the impact of crack interaction and loading scenarios on crack propagation. Our findings reveal that, initially, surface cracks grow independently, resembling single crack behavior. However, a pronounced interaction effect accelerates their growth as cracks propagate further, potentially leading to crack coalescence, high stress intensity factors, and reduced fatigue life. Consequently, this work highlights the need for integrating specific weld geometry representation in numerical models, as neglecting this can lead to significantly inaccurate fatigue life estimates in typical practical applications. Moreover, this study points out the challenge in accessing representative crack growth material parameters, vital for accurately evaluating the fatigue life of structural connections in offshore wind turbines.

KEYWORDS: Fatigue crack growth; stress intensity factor; crack interaction; crack coalescence; welded structures; offshore wind turbine foundations.

INTRODUCTION

The structural integrity of marine structures and other engineering systems is adversely influenced over their operational lifespan by deterioration mechanisms and mechanical stressors. In harsh marine environments exposed to corrosive agents such as saltwater and atmospheric contaminants, welding defects found in marine structures steadily propagate under cyclic loading induced by waves and other dynamic forces, making fatigue one of the main structural failure modes. In marine and offshore engineering communities, the fatigue assessment of welded structures is usually performed by relying on nominal stress S-N curves (DNVGL, 2016), yet the applicability of such S-N curves is constrained to structural configurations and loading conditions analogous to those in the original experimental setup.

A comprehensive modeling strategy entails the adoption of a linear elastic fracture mechanics (LEFM) approach for predicting the fatigue life of welded structures, particularly in scenarios that deviate from the experimental specimens used to establish conventional S-N curves. The crack growth modeled via LEFM is mainly governed by the stress intensity factor (SIF). This factor represents the stress field near the crack tip, derived from the crack size/geometry and applied loading. The fatigue crack growth of welded offshore steel structures can be modeled by a power law that establishes the relation between crack propagation rate, da/dN, and SIF range, ΔK (DNVGL, 2016; DNVGL, 2019). Naturally, suitable SIF solutions should be computed to yield accurate fatigue life predictions.

In real-world scenarios, welded sections often develop cracks because of the variation in material properties that is caused by the rapid heating and cooling cycles experienced during typical welding processes (Biswal et al., 2021). Due to the variation in material properties, the characterization of the stress field surrounding cracks originated from welded joints is a challenging task, where weld quality should be carefully considered, e.g., weld geometry, initial defects, residual stresses, and surrounding environment. Initial defects, commonly found near weldments, can rapidly propagate when subjected to cyclic loads owing to the local stress concentration at discontinuities. Consequently, the crack propagation prevails over the crack initiation phase (Wahab and Alam, 2004).

Additionally, the interaction between adjacent cracks and their potential coalescence should also be accounted for when predicting welded joints' fatigue life. Structural components often exhibit multiple adjacent surface cracks, and their behavior is influenced by various factors such as size, relative position, geometry, and applied stress. These interactions commonly hold significance in structures subjected to fatigue and stress corrosion cracking (Kamaya, 2005). Fatigue crack initiation and propagation experiments carried out for welded T-joints in offshore structural elements show that semi-elliptical cracks initiate along weld toes and may progressively coalesce, forming combined cracks (Bell and Vosikovsky, 1993). To study the influence of specimen thickness, stress distribution, and environment on the fatigue crack shape evolution, To et al. (1993) performed fatigue tests of welded T-plate, pipe-plate, and tubular joints. Their experimental campaign indicates that multiple cracks initiate along the weld toe early in the fatigue life, subsequently growing and potentially reaching coalescence, thereby resulting in a dominant crack. Similarly, Madia et al. (2017) show that micro-cracks at weld toe propagate individually and simultaneously until they eventually coalesce with neighboring cracks. As adjacent cracks approach each other, the interdependence of the stress field and SIFs lead to pronounced growth rates and complex crack shapes. Quantifying fatigue growth of adjacent surface cracks and their coalescence thus demands accounting for their mutual interactions. While SIF values for conventional welded joints are reported in standards such as BS7910 (2015); suitable SIF

solutions cannot, however, be easily found for structures with specific weld configurations, geometry, and/or loading conditions.

Since the nucleation of cracks along a weld toe is related to its notch geometry and the existence of micro-notches, weld toe local geometry at the weld toe plays a prominent role in the initiation of surface cracks (Madia et al., 2017). Weld geometry can be characterized by defining the weld toe angle, weld toe radius, width of weld reinforcement, height of reinforcement, and plate thickness. The effects of different welded geometry parameters on the fatigue life of welded joints are investigated by various researchers. For instance, Nguyen and Wahab (1993) investigated the effect of welding parameters on the SIF of welded joints. They developed an analytical model to predict the fatigue strength of welded joints subjected to the co-influence effect of butt-weld geometry parameters and demonstrated how weld profile geometry factors have a significant impact on the SIF. The effects of welding geometry on the fatigue properties of T-weld and cruciform joints loaded in tension and in bending were studied by Ferreira and Branco (2007) using finite element analysis. Plate thickness and welded toe radius were found to be the most significant factors influencing the fatigue characteristics of welded joints. Bowness and Lee (2000) proposed a set of equations for estimating weld toe magnification factors for semi-elliptical cracks in T–butt joints by considering different parameters such as crack depth and aspect ratios, attachment footprint, weld angle, and weld toe radius. The equations together with plain plate solutions of Newman and Raju (1981) can be used to compute the SIF solutions of T-butt joints. The fatigue life simulation results for butt welded joints by Schork et al. (2018) indicate that the effects of weld geometry become more significant toward the endurance limits. Furthermore, the effects of flank angle and toe radius are more significant than the effects of excess weld metal height within the simulated range. Recently, Kolios et al. (2019) proposed an approach based on combined three-dimensional laser scanning technology and finite element analysis (FEA) to accurately compute the stress concentration factor (SCF) in offshore welded structures specifically for circumferential weldments in offshore wind turbine (OWT) monopile foundations. They found that, depending on weld quality, the SCF at the weld toe varies significantly and ranges between 1.1 and 1.65. Additional fatigue testing using large dog-bone samples taken from 90 mm thick weldments showed cracks were initiated at areas of maximum stress concentration. Effective assessment of fatigue strength requires accurate modeling of the weld geometry as it influences the fatigue strength of welded joints.

In addition to the geometry at the weld toe, fatigue crack propagation is influenced by initial defect size and crack growth parameters too. The size and nature of weld defects significantly contribute to the initiation and subsequent propagation of cracks. Weld imperfections, such as slag inclusion at the weld toe, exist in all welded joints and act as pre-existing cracks and stress-raisers (Wahab and Alam, 2004). The identification and usage of appropriate crack growth parameters is also essential for the estimation of fatigue life of welded joints. Recommendations regarding the parameters to use in LEFM-based fatigue crack propagation models are specified in industrial standards (BS7910, 2015; Hobbacher, 2016; ABS, 2018; DNVGL, 2019). Hobbacher (2016) states that fatigue life estimates using LEFM approaches can be carried out with appropriate parameters and the calculations should be verified at known structural details; on the other hand, ABS (2018) and DNVGL (2019) propose that the assumptions for fracture mechanics analysis models can be calibrated by comparison with S-N models. In contrast, BS7910 (2015) recommends values for crack growth parameters that are appropriate for various materials and environments through a simple linear or bi-linear model to estimate the crack propagation in welded structures.

In a recent study, we propose a methodology that leverages three-dimensional finite element (FE) analysis to compute the SIF at any point along crack fronts, enabling a direct assessment of crack propagation under interaction effects (Mishael et al., 2023). A noteworthy feature of this methodology is its ability to adequately model the coalescence of adjacent cracks. Building upon this foundation, this work expands the scope by investigating the influence of welding effects on the progression of multiple adjacent cracks, specifically those located in circumferential welds commonly found in monopile-supported OWTs. A key addition is the explicit modeling of weld profiles within the underlying three-dimensional FE analysis. Additionally, we adopt a calibration approach based on industrial S-N curves to account for variability in crack growth parameters and initial crack size. This reliability-based calibration approach adheres to the methodology introduced by Hlaing et al. (2020) to determine crack growth parameters and initial crack size. Furthermore, we examine the impact of long-term stress range on crack propagation by comparing two approaches: (i) long-term stress range modeled as the expected value of a two-parameter Weibull distribution (DNVGL, 2019), and (ii) long-term stress range assumed as the equivalent stress range (Eurocode 3, 2005). In a practical case study, we investigate the propagation of two interacting surface cracks at the circumferential weld toe of a monopile-supported OWT, showcasing the effectiveness of our proposed approach.

FATIGUE CRACK GROWTH AND STRESS INTENSITY FACTOR

Crack growth modeling

Adhering to LEFM principles, crack propagation rate *da/dN*, can be numerically computed by solving the following ordinary differential equation:

$$\frac{da}{dN} = f(\Delta K, R, C), \tag{1}$$

where N represents the number of cycles, $R = \sigma_{min} / \sigma_{max}$ denotes stress ratio, i.e., minimum to maximum applied stress, and C is a material parameter usually derived from experimental data. Relevant industrial standards recommend Paris' law formulation for modeling fatigue crack growth in offshore structures (BS7910, 2015; DNVGL, 2019). Following Paris' law, two-dimensional crack growth can be calculated by solving a system of ordinary differential equations (Newman and Raju, 1981):

$$\frac{da}{dN} = C_a(\Delta K_a)^m; \tag{2}$$

$$\frac{dc}{dN} = C_c(\Delta K_c)^m, \tag{3}$$

where a and c are the crack depth and length of a surface crack idealized with semi-elliptical shape, ΔK_a and ΔK_c denote the stress intensity factor range at the crack deepest and surface points, and material and environmental effects are accounted for through the deterministic variables C_a, C_c, and m. To model crack growth retardation along the surface, Newman and Raju (1981) propose the use of distinct crack growth parameters, C_a, and C_c, each of which related to crack growth along the depth and surface directions, respectively. A relation between C_a, and C_c can be assumed as:

$$C_c = 0.9^m C_a, \tag{4}$$

where C_a and m parameters can be read from industrial standards (BS7910, 2015) or through calibration with respect to structural reliability estimates computed via damage accumulation Miner's rule (DNVGL, 2019; Hlaing et al., 2020).

If two or more surface cracks interact with each other, the stress intensity factors (SIFs) along their crack fronts become interdependent, thereby resulting in a combined crack growth propagation. In that case, the fatigue crack growth of multiple surface cracks can still be formulated by following Paris' law, yet specific SIF(s) should be considered for each crack:

$$\frac{da^{(i)}}{dN} = C_a(\Delta K_a^{(i)})^m \; ; \tag{5}$$

$$\frac{dc^{(i)}}{dN} = C_c(\Delta K_c^{(i)})^m \; , \tag{6}$$

where the superscript $i \in \{1, 2, \ldots, n\}$ represents an individual crack i out of n considered interacting surface cracks, and their combined propagation can be computed by numerically integrating da over a specific number of cycles, N, relying on methods such as Runge-Kutta.

Another aspect that demands careful consideration in interacting crack propagation modeling is the coalescence of multiple cracks. Interacting cracks may coalesce into a single crack during their growth as soon as their crack tips merge. During their coalescence, the crack shape largely deviates from the semi-elliptical profile that existed before coalescence. The coalesced crack forms a re-entrant (dented) portion at the contact point of the coalescing semi-elliptical surface cracks (Kamaya, 2008). Because of the greater SIF at the re-entrant portion, the re-entrant part of the coalesced crack front grows at a faster rate than the other areas, resulting in the formation of a semi-elliptical crack shape for the coalesced crack (Leek and Howard, 1996). Therefore, the coalesced crack can be modeled as a semi-elliptical surface crack with dimensions obtained from the combined geometry of the interacting cracks. It can also be assumed that the length of the new surface crack is equal to the sum of the lengths of the two previously interacting surface cracks, with its depth equal to the deepest crack before coalescence. Then, the crack growth can be calculated following Eqs. 2 and 3. This approach provides an initial estimate of crack growth under interaction and coalescence, even if the assumed crack re-characterization may lead to an overestimation of the actual crack growth.

Stress intensity factor for weld-toe surface cracks

As previously mentioned, the computation of fatigue crack growth requires an accurate estimation of stress intensity factor range, ΔK, which is analytically defined as:

$$\Delta K = \Delta\sigma\, Y(a,c)\sqrt{\pi a} \; , \tag{7}$$

where $\Delta\sigma$ corresponds to the applied stress range weighted by a shape factor, Y, that accounts for local geometrical and loading conditions, and is specified as a function of both crack depth, a, and crack length, c. Evaluating SIF range in practical scenarios presents a challenge due to its dependence with the crack depth and length, which undergoes continuous change during crack propagation. Nonetheless, existing works in literature offer closed-form analytical solutions that are predominantly applicable to standardized and idealized crack geometries under simplified loading conditions. For instance, a typical closed-form solution for the SIF range for surface cracks in a welded finite plate subjected to membrane and bending loading is formulated in DNVGL (2019) as:

$$\Delta K_a = \Delta\sigma\left[\alpha Y_{\mu a} M_{k\mu a} + (1-\alpha) Y_{ba} M_{kba}\right]\sqrt{\pi a} \; ; \tag{8}$$

$$\Delta K_c = \Delta\sigma\left[\alpha Y_{\mu c} M_{k\mu c} + (1-\alpha) Y_{bc} M_{kbc}\right]\sqrt{\pi a} \; , \tag{9}$$

where the subscripts μ and b stand for membrane and bending stress components. The factor α corresponds to the ratio between membrane and total stress and M_k represents the stress magnification factor accounting for the stress concentration due to local weld geometrical effects (Bowness and Lee, 2000). The geometric factors $Y_{\mu a}$, Y_{ba}, $Y_{\mu c}$, Y_{bc}, and stress magnification factors $M_{k\mu a}$, M_{kba}, $M_{k\mu c}$, M_{kbc} can be computed using the parametric equations listed in BS7910 (2015).

The parametric equations recommended by industrial standards (BS7910, 2015; DNVGL, 2019) are based on the magnification factors proposed by Bowness and Lee (2000) for 3D T-butt joints. However, M_k results for plate-to-plate butt welds differ from those for single T-butt joints (Lie et al., 2017). The percentage difference in values is as high as 63.8% for axial loading cases and 97.4% for bending loading cases. In addition, the intricate nature of cracked geometries and the complexity of service loads in practical scenarios render direct analytical solutions unattainable.

In contrast, numerical methods, such as finite element method (FEM), have proven useful for obtaining stress intensity factors in complex structures with irregular crack geometries. For instance, accepted stress intensity factor solutions for surface cracks on finite-thickness plates, hollow cylinders, and circular rods can be obtained via finite element analysis (Raju and Newman, 1979; Raju and Newman, 1986). Another approach involves combining numerical methods with existing solutions of weld geometry magnification factors proposed by standards such as DNVGL (2019). This will reduce the computational effort required to perform numerical simulations, especially when detailed information about weld geometry is not readily available. However, the efficacy of this approach relies on the determination and applicability of suitable weld geometry magnification factor solutions.

In this work, a three-dimensional FE model, following the approach proposed in our previous work (Mishael et al., 2023), is extended by considering the weld geometry, thus avoiding the need for parametric equations to compute the weld toe magnification factor (M_k) in practical scenarios, e.g., plate-to-plate butt-welded connections in offshore wind turbine monopile foundations. The accurate computation of SIF requires the development of appropriate finite element models that can represent semi-elliptical weld-toe cracks. Building upon our recent work on the finite element modeling scheme for semi-elliptical surface cracks (Mishael et al., 2023), we propose an alternative approach to model semi-elliptical weld-toe cracks. Recognizing the significance of the weld toe radius in creating a curved geometry near the weld toe, we adopt a modeling strategy that employs 10-node quadratic tetrahedral elements. These elements are chosen for their ability to accurately capture the complex features of surface cracks, especially in regions with curved geometries. Considering 10-node tetrahedral elements ensures an effective representation of the weld toe, addressing the challenges posed by its curved nature and contributing to the overall effectiveness of the FE model. They are also capable of automatically adapting to variations in crack dimensions during crack propagation. The semi-elliptical cracks located at the weld toe, along with their crack fronts, are carefully modeled using these quadratic tetrahedral elements. 8-node linear brick elements are used for creating a structured mesh for the remaining part of the model. The modeling procedure ensures that at least six contours

are available for the computation of SIF through the interaction integral method. Reasonably refined elements are used to model the semi-elliptical cracks, and sufficiently fine mesh is set up along the crack front to avoid the use of quarter-point elements.

Long-term stress range

The stress range influences the stress intensity factor, as shown in Eq. 1, and therefore, it is essential to consider long-term loading conditions in fatigue crack growth computations. For crack growth computations, offshore industrial standards (DNVGL, 2018; DNVGL, 2019) recommend using a long-term stress range described by a two-parameter Weibull distribution if long-term stress range data for the structure are not available. The exceedance probability derived from a two-parameter Weibull distribution can be represented as:

$$Q(\Delta\sigma) = exp\left[-\left(\frac{\Delta\sigma}{q}\right)^{h}\right], \tag{10}$$

where Q stands for the probability of exceedance corresponding to the stress range $\Delta\sigma$, while q and h are Weibull scale and shape parameters, respectively. The scale and shape parameters can be obtained from standards (DNVGL, 2016). To reduce the computational effort associated with three-dimensional finite element analysis, the expected value of the long-term stress range distribution is often employed in SIF computations. This approach provides a representative value that can be used to estimate the effects of long-term loading without the need for detailed and resource-intensive analyses.

An alternative approach for representing the long-term stress range is to use the equivalent constant amplitude stress range suggested in Eurocode 3 (2005), which is defined as the stress range that would result in the same fatigue life as the spectrum of variable amplitude stress ranges when the comparison is based on Palmgren-Miner's rule. The advantage of this approach lies in its ability to simplify the fatigue analysis by transforming variable amplitude loading scenarios into an equivalent constant amplitude, facilitating a more straightforward assessment of structural fatigue life. A simplified procedure for the determination of equivalent constant amplitude stress range is reported in Eurocode 3 (2005).

Initial crack size and crack growth parameters

The initial crack size influences the crack propagation life and plays a key role in the applicability of the LEFM approach. The calculated number of cycles is very sensitive to the dimensional parameters of the initial crack, especially for the crack depth (Hobbacher, 2011). Theoretical initial crack sizes can be determined by performing curve fitting based on experimental fatigue test data and crack growth parameters (Hobbacher, 2011). The initial crack size reported by researchers and suggested by standards varies between 0.1 and 0.5 mm. For instance, the crack size recommended by BS7608 (2015) ranges between 0.1 and 0.25 mm at the weld toe of flaw-free welded joints, whereas ABS standard (2018) suggests an initial crack depth of 0.5 mm for surface cracks starting from the transition between weld and base material. Radaj et al. (2006) suggest an initial crack depth greater than 0.15 mm and a surface crack length (2c) greater than 0.45-0.75 mm for the application of the LEFM approach. An initial crack depth of 0.1 mm is suggested by Lassen and Recho (2009) based on the inability for detecting cracks smaller than 0.1 mm during in-service inspections using non-destructive inspection techniques.

Crack growth parameters, C and m, are material dependent and usually derived from crack propagation experiments. They depend on many factors such as stress ratio, residual stress, environmental conditions, temperature, corrosion, among others. Hobbacher (2011) shows that there exists a large scatter in crack propagation data for different welded joints and recommended to set up an upper bound line for practical applications. However, in practical applications it is important to use the crack propagation parameters relevant to the specific material, loading, and environmental conditions under consideration. Mehmanparast et al. (2017) performed fatigue crack growth tests in air and seawater on S355G8+M steel, a widely used material in the fabrication of offshore wind monopile structures. Specifically, they proposed crack growth parameters for base metal as well as heat-affected zones in air and seawater (free-corrosion) environments. The investigation was motivated by the fact that available fatigue crack growth data for steels in air and seawater environments are several decades old and may not be appropriate for structural integrity assessment of offshore wind turbine foundations, which are fabricated using modern materials and welding technologies. In addition, crack growth data reported in offshore standards is based on the characteristics that are representative of typical offshore structures in the oil and gas industry. Instead of directly relying on material parameters listed in standards, it is also possible to estimate them by performing a calibration analysis that minimizes the difference in structural reliability with respect to estimates computed via Palmgren-Miner's rule (DNVGL, 2019; Hlaing et al., 2020, 2022).

This calibration process can be conceptualized as an optimization problem with the objective of minimizing the difference in estimated failure probabilities resulting from representative S-N data and the considered fracture mechanics model. Failure probability over time should be considered because, while fracture mechanics models compute crack growth evolution, S-N data only provides information about the failure or survival of the considered hotspot due to fatigue damage (DNVGL, 2019). The reader is advised to refer to Hlaing et al. (2022) for more information on the procedure to carry out the fracture mechanics parameter calibration based on a probabilistic approach. Alternatively, unknown fracture mechanics parameters can also be calibrated following a deterministic approach, by adjusting crack growth parameters so that through-thickness failure is reached at the same time as fatigue damage failure computed via Palmgren-Miner's rule and representative S-N data.

FATIGUE ANALYSIS OF INTERACTING SURFACE CRACKS IN OFFSHORE WIND WELDED CONNECTIONS

Case study description

In this case study, we investigate the influence of weld geometry, crack growth parameters, and long-term stress range approximations on the fatigue growth of interacting surface cracks that can be found in typical offshore wind monopile welded connections. We compare the propagation of two interacting cracks at the toe of a circumferential weld utilizing different methods to compute SIFs: (i) a finite element model considering both geometric and weld details, (ii) a finite element model where only geometric details are considered and relying on Bowness and Lee (2000) parametric equations to account for weld magnification effects, and (iii) computing geometric effects via Newman and Raju (1981) parametric equations along with Bowness and Lee (2000) magnification factors. Additionally, all experiments are compared against the growth of an independent single crack, where crack interaction effects are neglected.

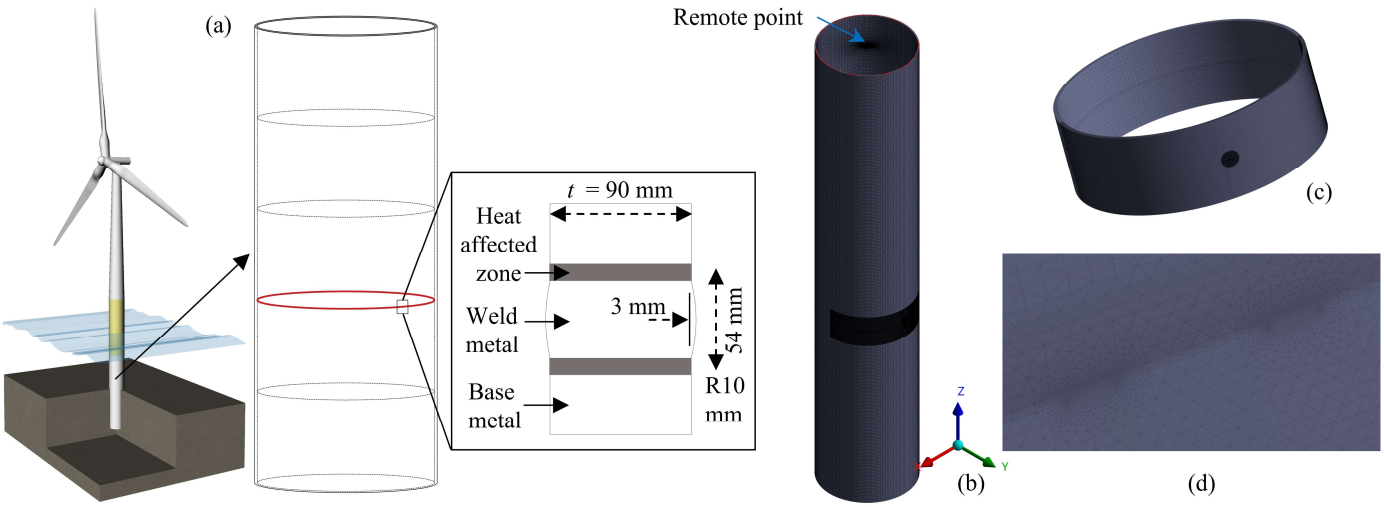

Fig. 1. Graphical representation of a typical offshore wind turbine monopile foundation, illustrating the studied weld geometry and its dimensions. (a) The examined surface cracks are located at the circumferential weld toe marked with a solid red line, (b) monopile FE model representation, also showcasing the remote point where the bending moment is applied, (c) local mesh near the circumferential weld region, and (d) refined mesh representation at the semi-elliptical cracks' location.

The subject of the study is a 30-m monopile substructure with a 3-m outer radius and a 90-mm wall thickness, t, installed in a water depth of 20 m. The examined structural detail corresponds to a monopile circumferential welded connection located at 12 m height from the seabed. The geometry of the weld and its dimensions are shown in Fig. 1. The monopile substructure is assumed to be made from S355 structural steel, which is a widely used material for the fabrication of offshore wind foundations (Mehmanparast et al., 2017). The modulus of elasticity and Poisson's ratio are specified as $2.1 \cdot 10^5$ MPa and 0.3, respectively. While not implemented in this work, one can additionally consider distinct material properties near the region of the weld, e.g., base metal, weld metal, and heat-affected zone. Adhering to typical practical scenarios (DNVGL, 2018), we set a service life of 20 years, in which the analyzed details experience approximately $7 \cdot 10^7$ stress cycles per year, caused by dynamic wind and wave loads (Dong et al., 2011).

Following the process suggested by industrial standards (DNVGL, 2016), initial crack size and crack growth parameters are calibrated as explained in the methodological section, considering a class D S-N curve, which is applicable to details exposed to seawater and equipped with cathodic protection. All resulting crack parameters are listed in Table 1, categorized according to the followed calibration approach (i.e., deterministic, or probabilistic), and based on the determined long-term stress range approximation. While it is interesting to observe the variation of the resulting crack parameters depending on the imposed assumptions, only the parameters calculated via the deterministic approach are considered in the experiments. This decision is made by considering computational efficiency and with preference on parameters that can be found in typical scenarios, as detailed in the previous section. An alternative approach one could instead adopt would be adjusting crack parameters according to the mean values resulting from the probabilistic calibration approach.

To study potential crack interaction effects, we model two identical surface cracks idealized with semi-elliptical geometries and separated by a distance-to-thickness ratio, $\delta/t = 0.09$, where δ is the distance between the semi-elliptical crack centers. The investigated surface cracks are analyzed under mode I fracture mode, which represents a critical fatigue failure mechanism commonly experienced by offshore wind structural components. To simulate the experienced combined wind and wave loads, a bending moment is applied at the top of the monopile FE model through a coupled remote point, as shown in Fig. 1.

Table 1. Initial crack size (a_0) and crack growth parameters (C) calibrated from Class D S-N curves in seawater with cathodic protection. The units corresponding to da/dN and ΔK are mm/cycle and MPa$\sqrt{\text{mm}}$, respectively.

Calibrated parameters	a_0 [mm]	C (mean)	C (standard deviation)	Approach
Expected stress range – 4.739 MPa				
a_0	2.8191	$3.4268 \cdot 10^{-13}$ (DNVGL, 2019)	0.22 (DNVGL, 2019)	Probabilistic
a_0 and C	0.5785	$8.5643 \cdot 10^{-13}$	0.56	Probabilistic
a_0	6.5797	$3.4268 \cdot 10^{-13}$ (DNVGL, 2019)	-	Deterministic
a_0 and C	**0.6895**	**$1.3239 \cdot 10^{-12}$**	**-**	**Deterministic**
Equivalent stress range – 17.052 MPa				
a_0	0.0037	$3.4268 \cdot 10^{-13}$ (DNVGL, 2019)	0.22 (DNVGL, 2019)	Probabilistic
a_0 and C	0.1525	$3.8667 \cdot 10^{-14}$	0.60	Probabilistic
a_0	0.0059	$3.4268 \cdot 10^{-13}$ (DNVGL, 2019)	-	Deterministic
a_0 and C	**0.5929**	**$3.0871 \cdot 10^{-14}$**	**-**	**Deterministic**

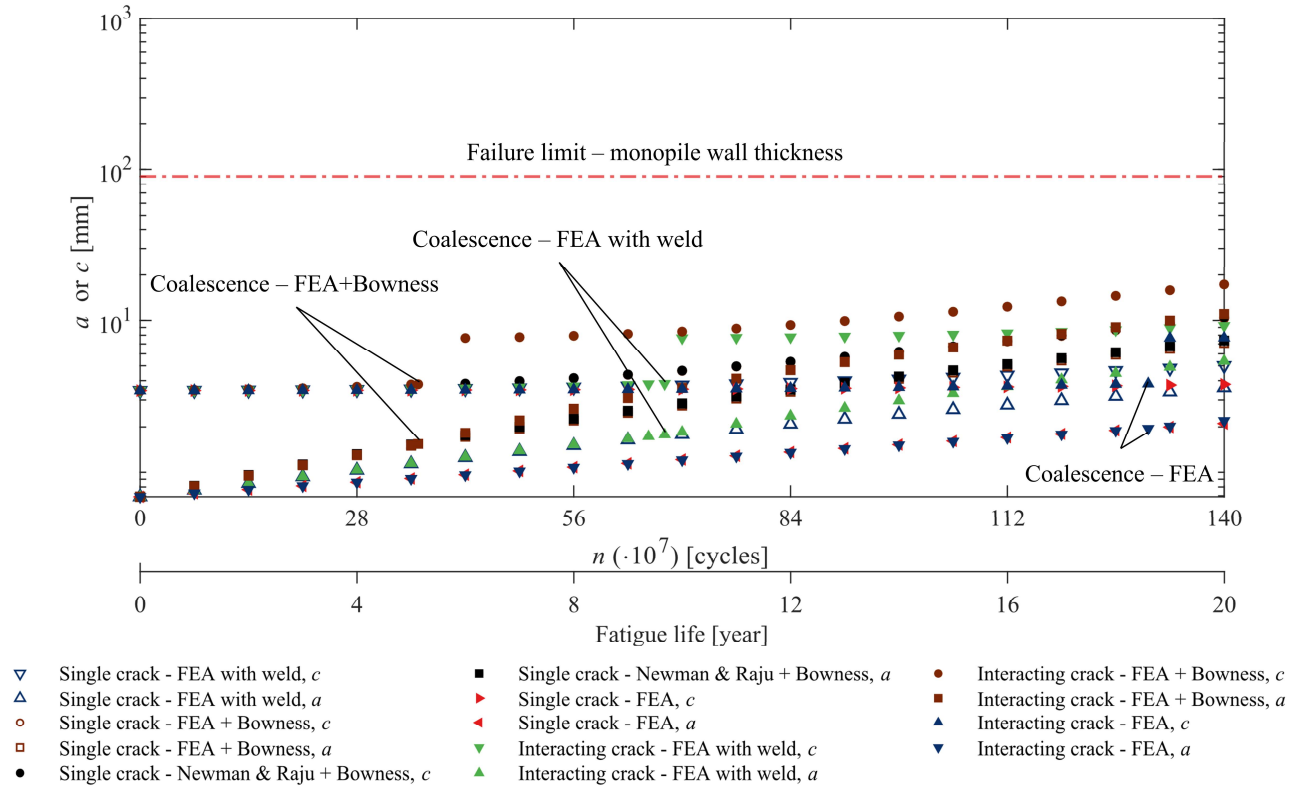

Fig. 2. Propagation of interacting cracks and independent single crack under expected stress range loading for all investigated methods.

Based on industrial standard recommendations (Eurocode 3, 2005; DNVGL, 2016), we examine two long-term stress range approximations in the numerical experiments, i.e., expected stress range and equivalent stress range, both explained in the previous section. The magnitudes of the considered stress ranges are 4.739 MPa and 17.052 MPa for expected and equivalent stress range, respectively. Furthermore, the monopile is assumed fixed to the seabed by restricting in the model all degrees of freedom at the bottom. The combination of a clamped boundary condition and applied bending moment induces a crack-opening effect at the investigated circumferential weld connection.

Results and discussion

The fatigue propagation experienced by a pair of interacting semi-elliptical cracks at the circumferential weld toe of a monopile foundation is illustrated in Fig. 2, where the growth of an independent single crack is also represented for comparison purposes. The investigated surface cracks grow almost independently during the early propagation stage since they are still far from each other, thus following the same path as an independent single crack. The stress field around each crack, at this initial phase, aligns with that of a single crack without inducing any notable stress concentration in the surrounding region. However, an interaction effect can be observed as the cracks continue to propagate over time, thereby resulting in a more pronounced crack growth compared to that of an independent crack. This interaction effect naturally becomes more prominent as the cracks draw closer to each other. The proximity of cracks induces a mutual influence, causing the stress fields around the cracks to overlap and interact. This phenomenon results in a collective rise in stress levels, marking the departure from stress distributions observed during the early, independent growth stage. This increase in stress levels is the primary cause for the pronounced crack growth observed in the later stage. Stress concentration zones induced by the cracks proximity further amplify the applied loading at the crack tips, leading to higher stress intensity factors (SIFs), thereby accelerating propagation of interacting surface cracks. When surface cracks draw near enough to each other, they coalesce into a single combined crack and continue to propagate until the end of the structural component's lifetime. The increased growth at this final stage can be attributed to elevated SIFs at both crack depth and surface points, which are induced by the increased crack area and aspect ratio that results from coalescence.

As shown in Fig. 2, the growth evolution of the investigated interacting cracks is clearly influenced by the weld profile, thus showing the importance of explicitly modeling weld effects in fatigue numerical simulations. As seen in the figure, cracks grow faster when weld geometry effects are considered, compared to the case where the weld geometry is not explicitly represented in the FE model. Interestingly, Fig. 2 also illustrates that accounting for weld geometry effects through Bowness and Lee magnification factors (Bowness and Lee, 2000) substantially overestimates crack growth in our numerical experiments. This behavior is observed for both interacting and independent cracks. A good agreement is, however, reached between the growth of a single crack derived from numerically computed SIFs and those based on published SIFs (Newman and Raju, 1981) if weld geometry effects are computed with Bowness and Lee magnification factors (Bowness and Lee, 2000) in both cases. This result verifies that the observed discrepancy is caused by the method used to account for weld effects. Specifically, the growth of an independent single crack significantly differs when SIFs are computed with either a FE model where the circumferential weld profile is incorporated or a FE model along with Bowness and Lee magnification factors (Bowness and Lee, 2000).

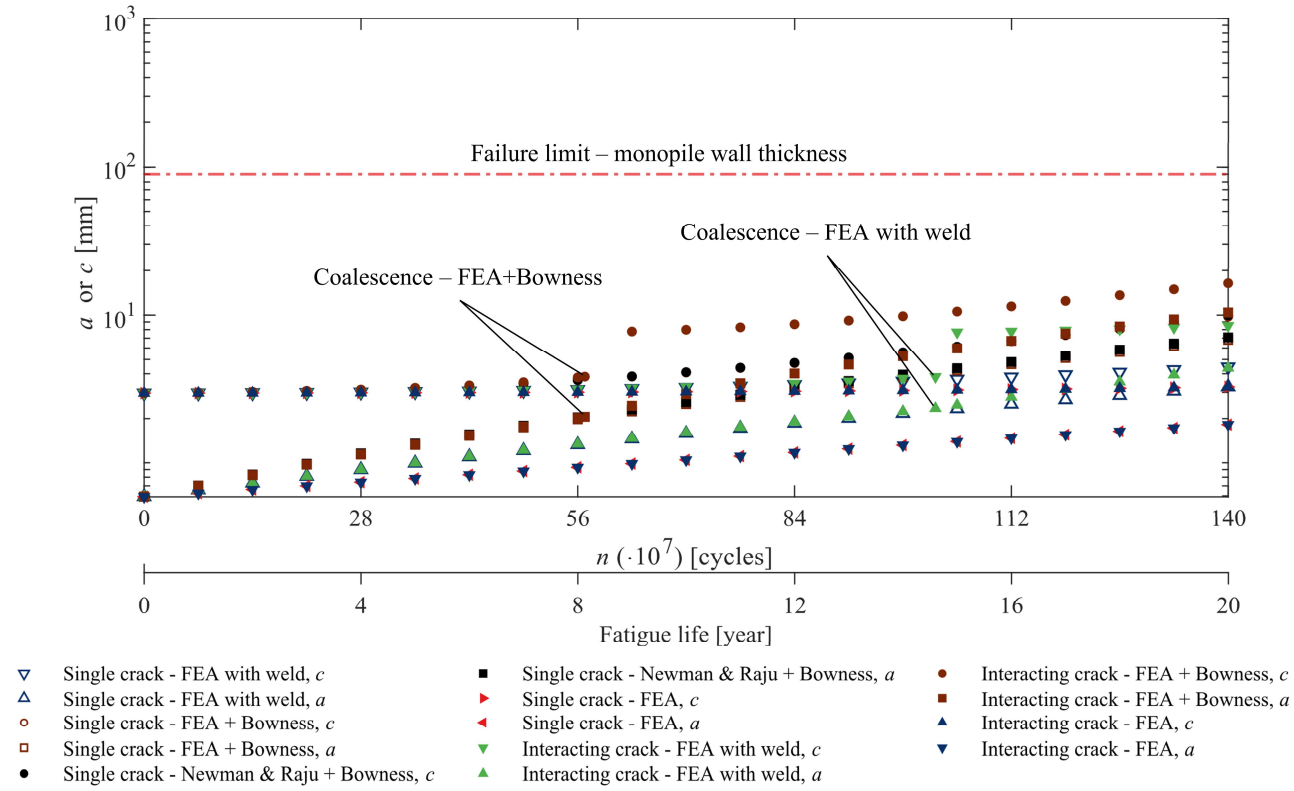

Fig. 3. Propagation of interacting cracks and independent single crack under equivalent stress range loading for all studied methods.

The difference in crack growth between these two modeling approaches is approximately 50% for both crack depth and surface points at the end of the service life of the studied monopile foundation.

Furthermore, the outcome from crack propagation numerical simulations for the case where long-term loading is approximated by an equivalent stress range is represented in Fig. 3. In this scenario, the discrepancy in the propagation of a single independent crack from a FE model where the circumferential weld is incorporated and the predicted growth when relying on parametric equations reaches up to 55% at the end of service life. A shift is, however, observed between the expected and equivalent stress range loading scenarios, mainly because the calibrated crack growth parameters are not equal, as shown in Table 1. The difference in the calibrated parameter values for all considered cases in Table 1 raises concern for effectively predicting the fatigue life of monopile foundations. Rational fatigue life predictions rely on crack growth parameters related to specific materials used in the offshore wind industry. Given that S-N curves currently available in standards mostly correspond to materials that are commonly used in the oil & gas industry, further research is needed to establish representative crack growth parameters for materials commonly employed in the offshore wind industry.

CONCLUSIONS

This study investigates the propagation of interacting surface cracks in circumferential welded connections of monopile-supported offshore wind turbines. Our findings highlight the importance of explicitly incorporating the geometry of weld profiles when numerically computing stress intensity factors. Relying simply on closed-form magnification factors may otherwise potentially lead to inaccurate fatigue life estimates in practical scenarios. Besides, the implementation of crack growth methods for evaluating the integrity of offshore wind structural connections is currently hindered by the unavailability of representative crack growth parameters. Future research directions are envisaged toward the development of probabilistic crack growth methods that account for variability in material parameters and initial crack size, while also effectively modeling crack interaction effects in offshore wind welded connections.

ACKNOWLEDGEMENTS

The authors gratefully acknowledge the financial support provided by the Belgian Energy Transition Fund (ETF) through the MAXWind project.

REFERENCES

ABS (2018). *Guide for Fatigue Assessment of Offshore Structures*, Standard, American Bureau of Shipping.

Bell, R, and Vosikovsky, O (1993). "Fatigue Life Prediction of Welded Joints for Offshore Structures Under Variable Amplitude Loading," *J. Offshore Mech. Arct. Eng*, 115, 123-130.

Biswal, R, Al Mamun, A, and Mehmanparast, A (2021). "On the performance of monopile weldments under service loading conditions and fatigue damage prediction," *Fatigue Fract Eng Mater Struct*, 44, 1-15.

Bowness, D, and Lee, M (2000). "Prediction of weld toe magnification factors for semi-elliptical cracks in T–butt joints," *Int J Fatigue*, 22, 369-387.

BS7608 (2015). *BS 7608:2014+A1:2015 - Guide to fatigue design and assessment of steel products*, Standard, British Standards Institution (BSI) Publication.
BS7910 (2015). *BS 7910:2013+A1:2015 - Guide to methods for assessing the acceptability of flaws in metallic structures*, Standard, British Standards Institution (BSI) Publication.
DNVGL (2016). *RP-C203 - Fatigue design of offshore steel structures*, Recommended Practice, DNV-GL.
DNVGL (2018). *ST-0126 - Support structures for wind turbines*, Standard, DNV-GL.
DNVGL (2019). *RP-C210 - Probabilistic methods for planning of inspection for fatigue cracks in offshore structures*, Recommended Practice, DNV-GL.
Dong, W, Moan, T, and Gao, Z (2011). "Long-term fatigue analysis of multi-planar tubular joints for jacket-type offshore wind turbine in time domain". *Eng Struct*, 33(6), 1-13.
Eurocode 3 (2005). *Eurocode 3: Design of steel structures - Part 1-9: Fatigue*, European Standard, EN 1993-1-9:2005, European Committee for Standardisation, Brussels.
Ferreira, J, and Branco, C (2007). "Fatigue analysis and prediction in fillet welded joints in the low thickness range". *Fatigue Fract Eng Mater Struct*, 13, 201-212.
Hlaing, N, Morato, PG, Nielsen, JS, Amirafshari, P, Kolios, A, and Rigo, P (2022). "Inspection and maintenance planning for offshore wind structural components: integrating fatigue failure criteria with Bayesian networks and Markov decision processes," *Struct Infrastruct Eng*, 18(7), 983-1001.
Hlaing, N, Morato, PG, Rigo, P, Amirafshari, P, Kolios, A, and Nielsen, JS (2020). "The effect of failure criteria on risk-based inspection planning of offshore wind support structures," *Proc. 7th Int Symp on Life-Cycle Civil Eng*, IALCCE, Shanghai, China.
Hobbacher, AF (2011). *Chapter 4 - The use of fracture mechanics in the fatigue analysis of welded joints*, in: Macdonald, KA (Ed.), *Fracture and Fatigue of Welded Joints and Structures*, Woodhead Publishing, Sawston, United Kingdom. 91-112.
Hobbacher, AF (2016). *Recommendations for Fatigue Design of Welded Joints and Components*, International Institute of Welding, Springer International Publishing, Switzerland.
Kamaya, M (2005). "Influence of the interaction on stress intensity factor of semi-elliptical surface cracks," *Proc ASME 2005 Pressure Vessels and Piping Conf*, Denver, Colorado, 3, 273-280.
Kamaya, M (2008). "Growth evaluation of multiple interacting surface cracks. Part I: Experiments and simulation of coalesced crack," *Eng Fract Mech*, 75, 1336-1349.
Kolios, A, Wang, L, Mehmanparast, A, and Brennan, F (2019). "Determination of stress concentration factors in offshore wind welded structures through a hybrid experimental and numerical approach," *Ocean Eng*, 178, 38-47.
Lassen, T, and Recho, N (2009). "Proposal for a more accurate physically based S-N curve for welded steel joints," *Int J Fatigue*, 31 (1), 70-78.
Leek, TH, and Howard, IC (1996). "An examination of methods of assessing interacting surface cracks by comparison with experimental data," *Int J Press Vessel Pip*, 68, 181-201.
Lie, ST, Zhao, HS, and Vipin, SP (2017). "New weld toe magnification factors for semi-elliptical cracks in plate-to-plate butt-welded joints," *Fatigue Fract Eng Mater Struct*, 40, 207-220.
Madia, M, Schork, B, Bernhard, J, and Kaffenberger, M (2017). "Multiple crack initiation and propagation in weldments under fatigue loading," *Procedia Structural Integrity*, 7, 423-430.
Mehmanparast, A, Brennan, F, and Tavares, I (2017). "Fatigue crack growth rates for offshore wind monopile weldments in air and seawater: SLIC inter-laboratory test results," *Mater Des*, 114, 494-504.
Mishael, J, Morato, PG, and Rigo, P (2023). "Numerical fatigue modeling and simulation of interacting surface cracks in offshore wind structural connections," *Mar Struct*, 92, 1-17.
Newman, JC, and Raju, IS (1981). "An empirical stress-intensity factor equation for the surface crack," *Eng Fract Mech*, 15, 185-192.
Nguyen, T, and Wahab, M (1993). "The effect of butt weld geometry parameters on stress intensity factor and fatigue life," *J. Comput. Mech*, 883-888.
Radaj, D, Sonsino, CM, and Fricke, W (2006). *Chapter 6 - Crack propagation approach for seam-welded joints*, in: Radaj, D, Sonsino, CM, and Fricke, W (Eds.), *Fatigue Assessment of Welded Joints by Local Approaches*, Woodhead Publishing, Sawston, United Kingdom, 233-295.
Raju, IS, and Newman, JC (1979). "Stress-intensity factors for a wide range of semi-elliptical surface cracks in finite-thickness plates," *Eng Fract Mech*, 11 (4), 817-829.
Raju, IS, and Newman, JC (1986). "Stress-intensity factors for circumferential surface cracks in pipes and rods under tension and bending loads," *Proc 17th National Symposium on Fracture Mechanics*, Albany, New York, 789-805.
Schork, B, Kucharczyk, P, Madia, M, Zerbst, U, Hensel, J, Bernhard, J, Tchuindjang, D, Kaffenberger, M, and Oechsner, M (2018). "The effect of the local and global weld geometry as well as material defects on crack initiation and fatigue strength," *Eng Fract Mech*, 198, 103-122.
To, S, Lambert, S, and Burns, D (1993). "A multiple crack model for fatigue in welded joints," *Int J Fatigue*, 15, 333-340.
Wahab, M, and Alam, M (2004). "The significance of weld imperfections and surface peening on fatigue crack propagation life of butt-welded joints," *J Mater Process Technol*, 153-154, 931-937.